Journal of Biomechanics 150 (2023) 111491

Contents lists available at ScienceDirect

Journal of Biomechanics

journal homepage: www.elsevier.com/locate/jbiomech

Blocking toll-like receptor 4 mitigates static loading induced pro-inflammatory expression in intervertebral disc motion segments

Hagar M. Kenawy [a], Samantha L. Marshall [b], James Rogot [a], Andy J. Lee [a], Clark T. Hung [a,b], Nadeen O. Chahine [a,b,*]

[a] Department of Biomedical Engineering, Columbia University, New York, NY, USA
[b] Department of Orthopedic Surgery, Columbia University Irving Medical Center, New York, NY, USA

ARTICLE INFO

Keywords:
Intervertebral disc
Degenerative disc model
Mechanical loading
Static
Dynamic
Inflammation
Cytokines
TAK-242
Tlr4
Hmgb1

ABSTRACT

While the anabolic effects of mechanical loading on the intervertebral disc (IVD) have been extensively studied, inflammatory responses to loading have not been as well characterized. Recent studies have highlighted a significant role of innate immune activation, particularly that of toll-like receptors (TLRs), in IVD degeneration. Biological responses of intervertebral disc cells to loading depend on many factors that include magnitude and frequency. The goals of this study were to characterize the inflammatory signaling changes in response to static and dynamic loading of IVD and investigate the contributions of TLR4 signaling in response to mechanical loading. Rat bone-disc-bone motion segments were loaded for 3 hr under a static load (20 % strain, 0 Hz) with or without an additional low-dynamic (4 % dynamic strain, 0.5 Hz) or high-dynamic (8 % dynamic strain, 3 Hz) strain, and results were compared to unloaded controls. Some samples were also loaded with or without TAK-242, an inhibitor of TLR4 signaling. The magnitude of NO release into the loading media (LM) was correlated with the applied frequency and strain magnitudes across different loading groups. Injurious loading profiles, such as static and high-dynamic, significantly increased *Tlr4* and *Hmgb1* expression while this result was not observed in the more physiologically relevant low-dynamic loading group. TAK-242 co-treatment decreased pro-inflammatory expression in static but not dynamic loaded groups, suggesting that TLR4 plays a direct role in mediating inflammatory responses of IVD to static compression. Overall, the microenvironment induced by dynamic loading diminished the protective effects of the TAK-242, suggesting that TLR4 plays a direct role in mediating inflammatory responses of IVD to static loading injury.

1. Introduction

Degeneration of the intervertebral disc (IVD), the soft connective tissue between spinal vertebrae, is often associated with low back pain (LBP). LBP is a common condition, affecting at least 266 million individuals worldwide (Frymoyer & Cats-Baril, 1991; Ravindra et al., 2018). The IVD is normally exposed to multimodal loading (e.g., compression, tension, shear, hydrostatic pressure, and osmotic pressure (Baer et al., 2003; Best et al., 1994; Gu & Yao, 2003; Iatridis et al., 1998; Nachemson, 1981; Wilke et al., 1999). It is estimated that human lumbar motion discs experience 4.4–6.7 % axial strain (O'Connell et al., 2007; O'Connell et al., 2011) and intradiscal pressures ranging from 0.03 to 0.7 MPa (Schultz et al., 1979; Wilke et al., 1999) under physiologic conditions. However, both frequency and magnitude regulate whether loading is beneficial or detrimental to disc integrity (MacLean et al., 2004, 2005; Walsh & Lotz, 2004; Wuertz et al., 2009). Static loading associated with sedentary posture or dynamic activities that involve high-frequency loading (e.g. motor vehicle or aircraft operators) have higher incidence of LBP (Christ & Dupuis, 1966; Dunstan et al., 2012; Healy et al., 2011; Magnusson, 1992; Matthews et al., 2008; Pope et al., 1998; Sandover, 1983; Wilder & Pope, 1996). This may be related to the variable response of the IVD to different loading profiles.

It is also well established that loading profiles regulate IVD cell response in a magnitude and frequency dependent manner, where prolonged static loading or dynamic loading above 1 Hz promotes matrix degradation *in vivo*, and loading at or below 0.5 Hz exhibits anabolic effects on the disc (Huang & Gu, 2008; Lang et al., 2018; Le Maitre et al., 2008; Le Maitre et al., 2009; MacLean et al., 2004; MacLean et al., 2003; Salvatierra et al., 2011; Setton & Chen, 2006; Wuertz et al., 2009; Yao & Gu, 2006). While the anabolic effects of mechanical loading on the IVD

* Corresponding author at: Department of Orthopedic Surgery, Columbia University, 650 West 168th Street, 1408E, New York, NY 10032, USA.
E-mail address: noc7@columbia.edu (N.O. Chahine).

https://doi.org/10.1016/j.jbiomech.2023.111491
Accepted 8 February 2023
Available online 11 February 2023

have been extensively studied *in vitro*, resulting inflammatory cascades have not been well characterized, although studies suggest that they are also influenced by the loading profile (Korecki et al., 2009; Wang et al., 2007; Wuertz et al., 2009). Nucleus pulposus (NP) cells secreted interleukin 1β (IL-1β) and tumor necrosis factor-α (TNFα) and upregulated matrix related genes Type-II-collagen (COL2A1), aggrecan (ACAN), and matrix metalloproteinase-3 (MMP3) in response to compressive loading (Korecki et al., 2009; Wang et al., 2007; Wuertz et al., 2009). Zhou *et al.* compressed bovine caudal discs 50 % of IVD height using a single injurious insult and saw increases in MMP expression and NO release versus physiological loading (Zhou et al., 2021). Additionally, they observed greater inflammatory responses at 1-day post loading versus 8-days post loading. Nevertheless, changes in inflammatory cytokine profiles of whole bone-disc-bone motion segments in response to loading remain understudied.

Recent studies have highlighted a significant role of innate immune activation, particularly toll-like receptors (TLRs) in IVD degeneration (Klawitter et al., 2014; Maidhof et al., 2014; Quero et al., 2013; Rajan et al., 2013). TLR4 is involved in the pathogenesis of the IVD, where expression of TLR4 increases with increasing degeneration severity and mediates catabolic and inflammatory processes (Klawitter et al., 2014; Maidhof et al., 2014; Quero et al., 2013; Rajan et al., 2013). Activation of TLR4 has been shown to induce a pro-inflammatory cascade in IVD cells with subsequent loss of IVD matrix integrity (Rajan et al., 2013). Additionally, damage associated matrix patterns, such as high-mobility group box-1 (HMGB1), have degenerative effects on disc cells mediated by TLR signaling (Krock et al., 2017; Shah et al., 2019). Furthermore, HMGB1 signaling increases expression of TLR4 suggesting a possible feedback signal (Fang & Jiang, 2016). While these studies identify TLR4 to be a critical regulator of joint pathology, the potential contribution of TLR4 to mechanically-induced inflammatory signaling of the IVD is unknown.

The goals of this study were to characterize the inflammatory signaling changes in response to IVD static and dynamic loading and investigate contributions of TLR4 signaling in response to mechanical loading. We hypothesized that loading profiles would modulate the inflammatory response depending on frequency and amplitude, and that TAK-242, a small molecule inhibitor of TLR4 signaling, would reduce pro-inflammatory signaling and promote anti-inflammatory gene expression. Thus, bone-disc-bone motion segments were used in a loading organ culture model to characterize IVD morphological, inflammatory, and histological responses when subjected to distinct loading profiles with and without TAK-242.

2. Materials and methods (Table S.1 for suppliers)

2.1. Sample isolation and tissue culture of discs

Caudal (Coccygeal/Co) bone-disc-bone motion segments (N = 104) were isolated from 26 mature male Sprague-Dawley rats (300 – 500 g). Segments were allocated consistently by level, unloaded: Co13-Co14, static: Co11-Co12, low dynamic: Co12-Co13, and high-dynamic: Co10-Co11, and washed in 1x PBS with 1 % antibiotic–antimycotic (AA) (Fig. 1**A**). Cuts were made mid vertebral body to separate levels, and samples were submerged in Dulbecco's Modified Eagle Medium (DMEM) containing 10 % FBS and 1 % antibiotics/antimycotics (AA). Motion segments were then cultured in chemically defined media (CM: phenol-free DMEM without L-glutamine, 100 μg/mL sodium pyruvate, 50 μg/mL L-proline, 1 % AA and 1 % ITS Premix) (Kelly et al., 2008).

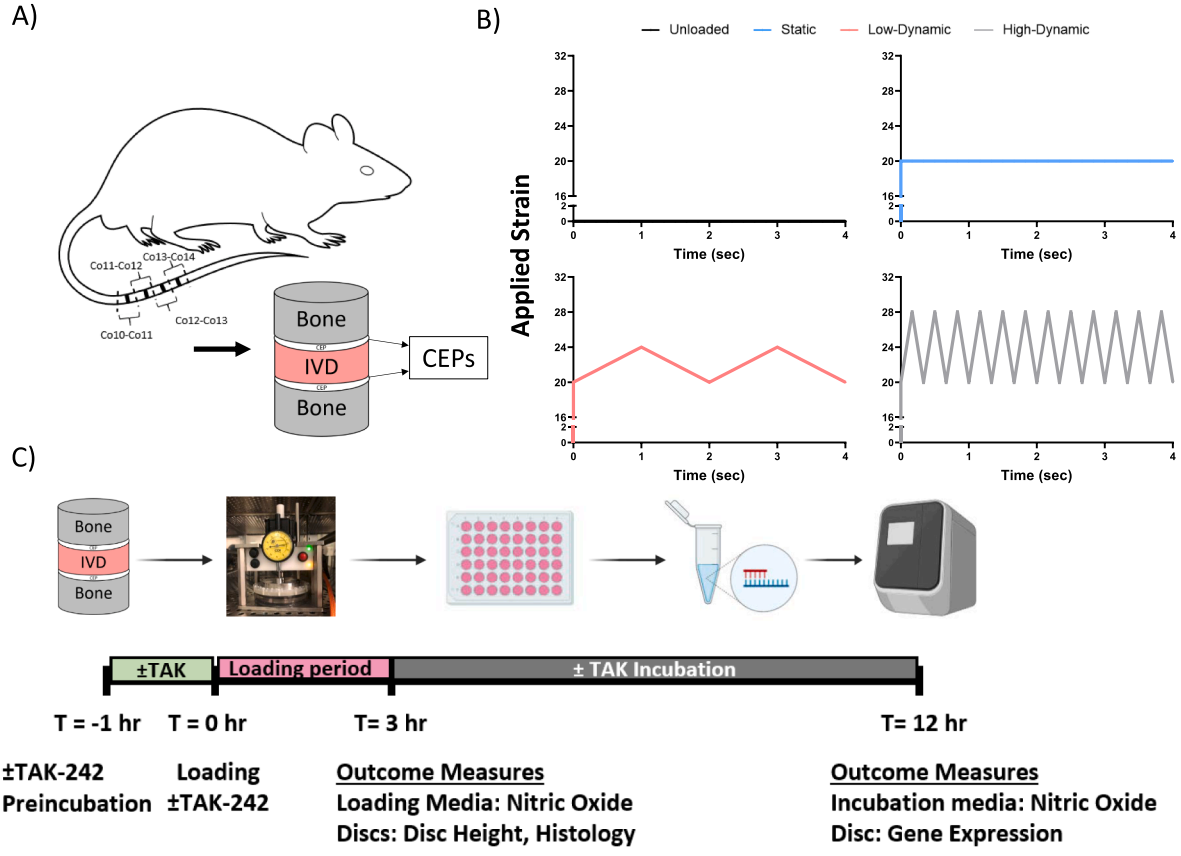

Fig. 1. Experimental methods. A) Dissection of caudal (bone-IVD-bone) motion segments with intact cartilage end plates (CEPs) from male Sprague-Dawley rats. **B)** Loading profiles applied to motion segments for a duration of 3 hr. **C)** Timeline and study design.

2.2. Loading conditions

Samples were loaded for 3 hr using a custom-made displacement control device (**Table S.2**) to apply static and dynamic loading profiles, with varying magnitudes and frequencies (Fig. 1**B**). A tare compressive strain of ~ 20 % of segment height (1.75 mm) was applied to the static group to retain contact between the loading platen and sample, eliminating liftoff. The low- and high-dynamic groups were loaded with a 20 % static strain plus an additional dynamic strain (low-dynamic: 4 % dynamic strain (0.35 mm) applied at 0.5 Hz, high-dynamic: 8 % dynamic strain (0.70 mm) applied at 3 Hz). Unloaded segments were cultured as free-swelling controls. To assess whether inflammatory signaling persists with recurring, long-term loading, a group of samples was loaded daily using the above protocol for 5-days (**Fig.S1,S2**). To assess the effect of applied strain magnitude on responses, we also compared samples loaded under static protocol with samples loaded under a high-static strain protocol (20 % tare + additional 8 % static strain) (**Fig.S4**).

Three segments were loaded simultaneously while submerged in CM. After collecting loading media (LM), motion segments were then transferred to individual wells and incubated with fresh CM for 9 hr. Individual sample incubation media was collected for analysis. IVDs were snap-frozen, after removal of adjacent vertebrae, for RNA extraction. Greiss Reagent System Assay was used to measure NO levels in loading and incubation media.

2.3. Disc height changes

Radiographic analysis of IVDs was performed using a BenchTop Labscope. Pre- and post-loading images were acquired, and disc height change from pre-load to post-load for each sample was analyzed using ImageJ (Schneider et al., 2012). Five equally-spaced measurements were taken across the width for each sample and averaged to compute disc height change (%).

2.4. TLR4 inhibitor (TAK-242)

TAK-242, or Resatorvid, was dissolved in DMF and further diluted in media. A pilot study was conducted to identify an efficacious TAK-242 dose for IVD motion segments. Control segments were cultured with LPS (1 μg/ml) with or without TAK-242 (at 1 or 10 μM) for 24 hr. Resulting NO release into the media informed the TAK-242 dosing selected for loaded IVDs samples. Segments were incubated with TAK-242 at 1.0 μM throughout the experiment, starting from 1 hr prior to loading, to during loading, and during 9 hr post-loading incubation (Fig. 1**C**).

2.5. Histology

To evaluate changes in IVD morphology, a subset of samples was fixed in 10 % buffered formalin phosphate overnight at 4 °C and stored in 70 % ethanol. Motion segments were decalcified in EDTA for two weeks. Decalcified discs were paraffin-embedded and sectioned (7 μm). Slides were stained with Alcian Blue (pH = 1.0, glycosaminoglycan (GAG)), Picrosirius Red (collagen), and H&E (cellularity). Images were taken using a Zeiss Axio Observer Z1 using Axiocam 503 color camera.

2.6. qPCR preparation

For RNA extraction, IVD tissues were minced and processed with TRIzol, and a stick homogenizer followed by phase-lock separation. RNA precipitation was performed using Qiagen miRNeasy columns. cDNA was synthesized using iScript cDNA Synthesis Kit. Gene specific master mixes were prepared using designed primers (Table 1) and iTaq Universal SYBR Green Supermix. RT-qPCR was run on a QuantStudio™ 6 Flex Real-Time PCR System. *Gapdh* was used as the housekeeping gene.

Table 1
qPCR Primer Sequences.

Gene	FWD Primer Sequence	REV Primer Sequence	Amplicon Size (bp)
Acan	GGA TCT ATC GGT GTG AAG TGA TG	AGT GTG TAG CGT GTG GAA ATA G	112
Arg1	CCA AGC CAA AGC CCA TAG A	CCA GGC CAG CTT TCC TTA AT	102
Col1a1	GCT TGA AGA CCT ATG TGG GTA TAA	GGG TGG AGA AAG GAA CAG AAA	89
Col2a1	CAT AGG GCC TGT CTG TTT CTT	CCA TTC AGT GCA GAT CCT AGA G	117
Gapdh	GCA AGG ATA CTG AGA GCA AGA G	GGA TGG AAT TGT GAG GGA GAT G	98
Hmgb1	TCG GCC TTC TTC TTG TTC TG	GTT GTT CCA CAT CTC TCC TAG TT	108
Ifng	GTG AAC AAC CCA CAG ATC CA	GAA TCA GCA CCG ACT CCT TT	111
Il10	CTG CAG GAC TTT AAG GGT TAC T	TTT CTG GGC CAT GGT TCT C	103
Il1b	TCT GAC AGG CAA CCA CTT AC	CAT CCC ATA CAC ACG GAC AA	128
Il6	GAA GTT AGA GTC ACA GAA GGA GTG	GTT TGC CGA GTA GAC CTC ATA G	105
Mmp3	CCT GAT AGC TCT TCC TCT GAA AC	GGT TGA CTG GTG CCA TAT GTA	104
Mmp12	CTG GTT CGG TTG TTA GGA AGA	CCC TGA GCA TAC AGT GGA TAT G	90
Nos2	CAA CTA CTG CTG GTG GTT ACA	AAG GTA TGC CCG AGT TCT TTC	107
Tlr4	CAG AGC CGT TGG TGT ATC TT	AGC AAG GAC TTC TCC ACT TTC	110
Tnfa	CCC AAT CTG TGT CCT TCT AAC T	CAG CGT CTC GTG TGT TTC T	105

Samples were normalized to the unloaded controls without TAK-242 using $2^{-\Delta\Delta Ct}$ method (Fig. 1**C**).

2.7. Statistics

One-way ANOVAs with Holm-Sidak post-hoc tests were conducted comparing changes in disc height and NO release into LM. Spearman correlations were conducted to analyze the effects of applied strain and frequency on NO release into LM. Student t-tests were conducted on gene expression of loaded versus unloaded discs. Student t-tests were also conducted to compare the effect of TAK-242 in each loading group versus the no TAK-242 analog. Kruskal-Wallis and Mann-Whitney non-parametric tests were used with non-normal data as indicated by the Shapiro-Wilk test. Outliers were detected using robust regression and outlier removal (ROUT) method with a maximum desired False Discovery Rate (Q) of 1 % (Motulsky and Brown, 2006). Statistical significance was set at $^{*}p < 0.05$ where $\alpha = 0.05$, and any trends where $^{\#}p < 0.1$ were noted, from analyses performed uisng GraphPad Prism 9.2.0.

3. Results

3.1. IVD height changes with loading

The average disc height increased by 8.5 ± 9 % in unloaded samples. Disc height significantly decreased by 17 ± 12 %, 36 ± 22 %, and 61 ± 13 % in static ($p = 0.001$), low-dynamic ($p < 1.0 \times 10^{-4}$), and high-dynamic ($p < 1.0 \times 10^{-4}$) groups, respectively, versus unloaded group (Fig. 2**E**). Disc height change in high-dynamic was significantly greater than low-dynamic ($p = 0.012$) and static ($p < 1.0 \times 10^{-4}$), which were also different from each other ($p = 0.022$).

3.2. NO and gene expression of loaded IVDs

NO release into low-dynamic ($p = 0.016$) and high-dynamic ($p < 1.0 \times 10^{-4}$) LM was significantly higher compared to unloaded (Fig. 3**A**). NO

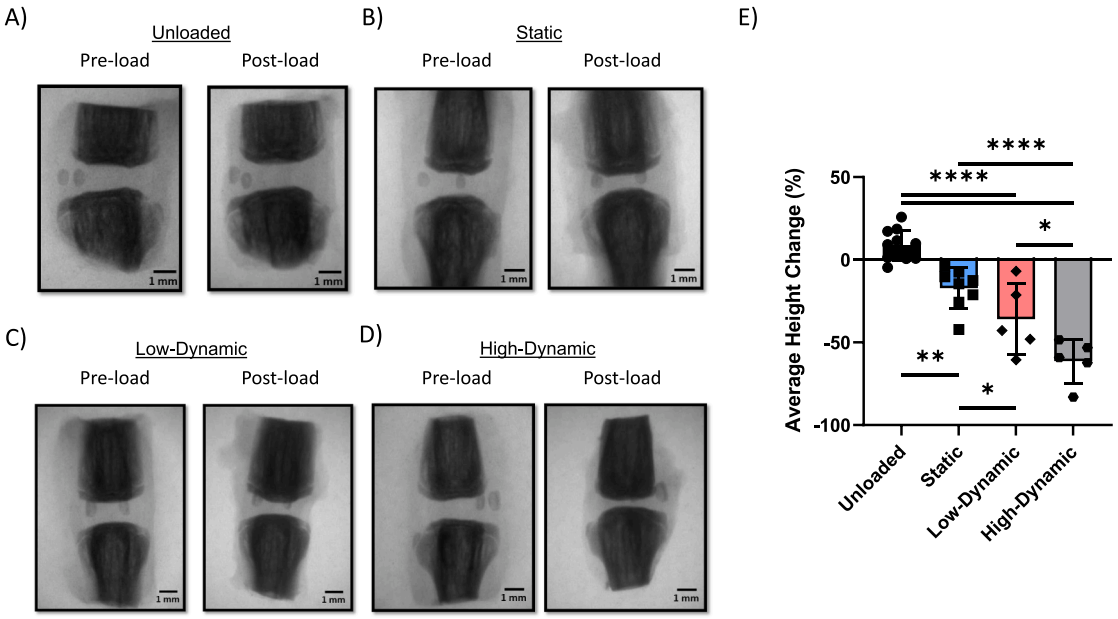

Fig. 2. Disc height analysis at 3 hr post loading. Representative fluoroscope images of **A)** an unloaded motion segment , **B)** a static loaded motion segment, **C)** a low-dynamic loaded motion segment, and **D)** a high-dynamic loaded motion segment acquired pre- and post-load. **E)** Average IVD height change (%) under each loading profile (N = 11,8,5,5, respectively). ****$p < 0.0001$, **$p < 0.01$, and *$p < 0.05$.

release during static loading was significantly lower compared to low- ($p = 0.016$) and high-dynamic loading ($p < 1.0 \times 10^{-4}$). Low-dynamic loading released less NO than high-dynamic loading ($p = 0.017$) (Fig. 3**A**). NO release during loading was dependent on both applied strain ($p < 1.0 \times 10^{-4}$, $r = 0.86$) and frequency ($p < 1.0 \times 10^{-4}$, $r = 0.89$) (Fig. 3**Bi-ii.**). There were no differences in NO release from individual discs during incubation ($p = 0.67$) (Fig. 3**C**). In the 5-day loading study, cumulative NO levels increased at a greater rate in high-dynamic versus static, where both loading profiles resulted in increased NO versus unloaded **(Fig.S1)**.

When looking at gene expression in loaded IVDs, pro-inflammatory genes *Nos2* ($p = 0.025$), *Tnfa* ($p = 1.0 \times 10^{-4}$), and *Il1b* ($p = 0.020$) were upregulated in the high-dynamic loaded discs versus unloaded. *Tlr4* ($p = 0.028$) and *Hmgb1* ($p = 3.0 \times 10^{-4}$) expression also increased in high-dynamic group versus unloaded. Anti-inflammatory *Il10* ($p = 0.0036$) and *Arg1* ($p = 0.023$) expression also significantly increased in high-dynamic versus unloaded (Fig. 3**D-F,H-I,K-L).** Expression of ECM genes *Col1a1* ($p = 0.032$), *Col2a1* ($p = 0.0019$), *Acan* ($p = 0.0011$), and *Mmp3* ($p = 0.030$) was downregulated in high-dynamic loading versus unloaded discs (Fig. 3**M**). Under static loading, gene expression of *Nos2* ($p = 0.030$), *Tnfa* ($p = 0.0026$), *Il1b* ($p = 0.046$), *Ifng* ($p = 0.0098$), *Tlr4* ($p = 0.012$), *Hmgb1* ($p = 0.0079$), *Il10* ($p = 0.0073$), and *Arg1* ($p = 0.017$), was upregulated versus unloaded discs (Fig. 3**D-F,H,I,K,L**). Expression of *Col1a1* ($p = 0.0071$), *Col2a1* ($p = 0.0022$), *Acan* ($p = 8.0 \times 10^{-4}$), and *Mmp3* ($p = 0.018$) was also downregulated under static loading versus unloaded (Fig. 3**M**). Low-dynamic loading had significantly lower expression of *Arg1* ($p = 0.033$) and *Acan* ($p = 0.032$) versus unloaded (Fig. 3**L,M**). Overall, inflammatory gene expression was more upregulated in response to 1-day of loading, when compared to 5-day loading, and inhibition in ECM gene expression due to loading appeared to recover with 5-day loading (**Fig.S1,S2**), suggesting that 5-day loading simulated IVD remodeling.

3.3. Effects of TAK-242 on loading response

In unloaded discs stimulated with LPS, TAK-242 reduced NO production at both 1 and 10 μM ($p = 0.0020$) (Fig. 4**A**). The addition of TAK-242 to the media of the unloaded discs did not affect NO release in the first 3 hr ($p = 0.23$) (Fig. 4**B**), but it reduced subsequent NO release in the incubation media ($p = 2.0 \times 10^{-4}$) (Fig. 4**C**). Unloaded + TAK242 significantly decreased *Il6* ($p = 0.0023$) and *Arg1* ($p = 0.027$) versus unloaded discs (Fig. 4**D**). ECM genes *Col1a1* ($p = 0.037$), *Col2a1* ($p = 0.0037$), and *Acan* ($p = 0.0028$) were also significantly downregulated (Fig. 4**E**).

TAK-242 did not alter NO release into the static LM ($p = 0.26$) (Fig. 5**A**), but reduced NO release into the post static loading incubation media ($p = 0.021$) (Fig. 5**B**). *Tlr4* ($p = 0.018$), *Tnfa* ($p = 0.020$), and *Ifng* ($p = 0.010$) expression significantly decreased in static + TAK242 versus static (Fig. 5**C**). *Arg1* ($p = 0.039$), *Col1a1* ($p = 0.0079$), *Col2a1* ($p = 0.026$), *Acan* ($p = 0.016$), *Mmp3* ($p = 0.0065$), and *Mmp12* ($p = 0.045$) expression significantly increased in static + TAK242 versus static (Fig. 5**C-D**).

During low- and high-dynamic loading, NO release into LM ($p = 0.81$, $p = 0.85$) (Fig. 5**E,I**) and incubation media ($p = 0.22$, $p = 0.22$) (Fig. 5**F,J**) was not significantly different from their no TAK-242 counterparts. However, there were significant increases in *Il6* ($p = 0.0063$) and *Arg1* ($p = 9.5 \times 10^{-4}$) gene expression in high-dynamic + TAK242 versus high-dynamic (Fig. 5**K**).

3.4. Histology

In unloaded discs, the NP appeared round and constituted much of the disc cross-sectional area (Fig. 6**A-C**). About 80 % of NP cells were large and vacuolated, surrounded by a GAG-rich matrix (Fig. 6**D**). The NP-AF border was distinct (Fig. 6**A-C**). The AF was composed of well-organized collagen-rich discrete lamellae bulging outward (Fig. 6**E**). Under static loading, the NP region appeared compacted and displaced by AF-like collagen matrix, with little evidence of NP vacuolated cells (Fig. 6**D**). The AF lamellae were distorted (serpentine) or ruptured, and the NP-AF border was indistinguishable (Fig. 6**E**). In low- and high-dynamic groups, the NP appeared round but asymmetric and convex (Fig. 6**D**), with a pronounced irregular shape observed in high-dynamic. Fewer clustered vacuolated cells were observed in low-dynamic versus unloaded, while the AF appeared to be distorted, with observations of lamella infolding and NP-AF border disruptions (Fig. 6**A-C**). In high-dynamic, the NP was full of GAG-rich clusters and was surrounded by a mildly disrupted inner AF (Fig. 6**D**). The outer AF exhibited disruption in collagen lamellae with increased fissures (Fig. 6**E**).

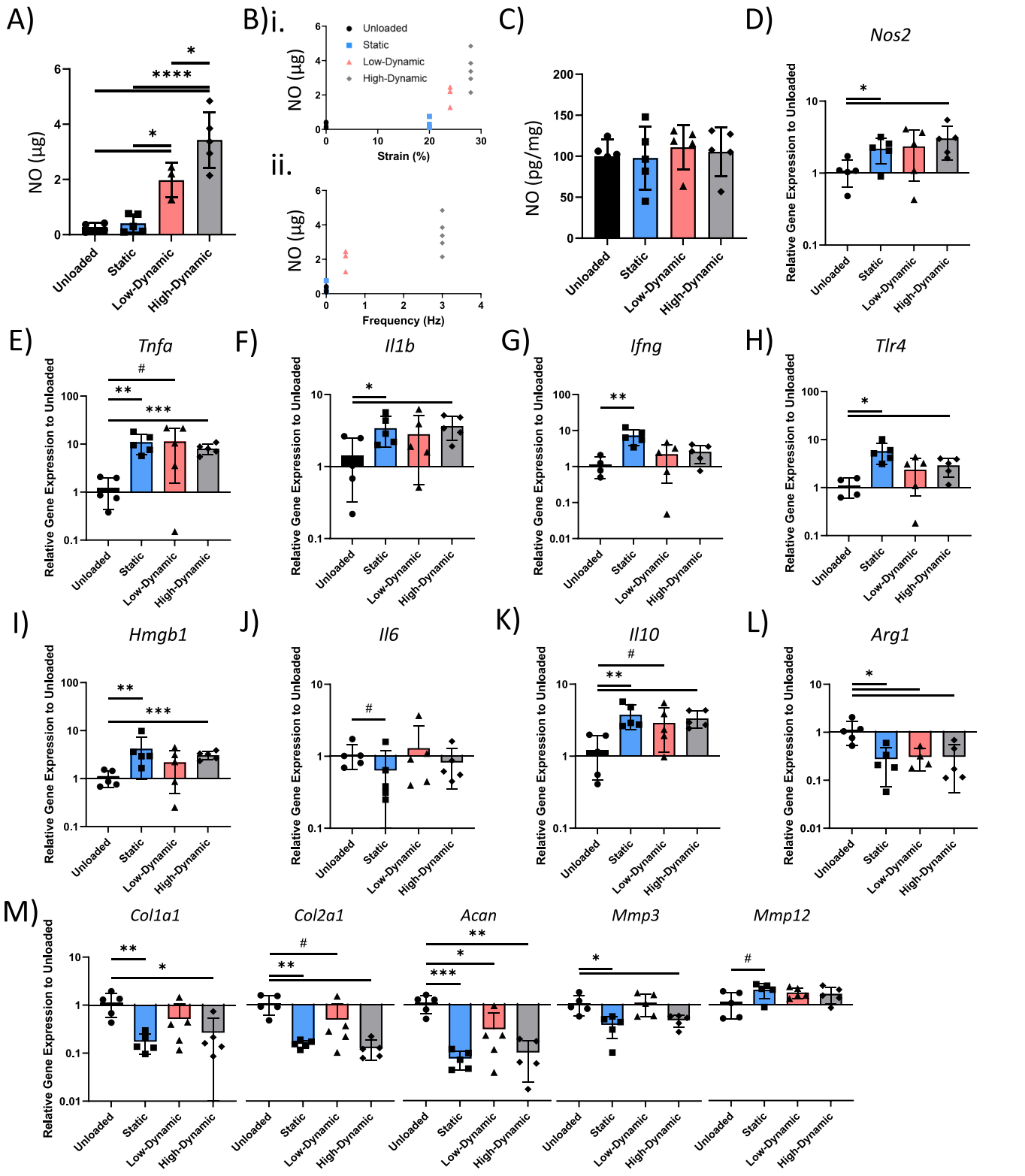

Fig. 3. Inflammatory cytokine profiles of loaded discs. A) NO released into loading media of unloaded, static, low-dynamic, and high-dynamic conditions (N = 4,3,3,5), **B)** NO release as a function of applied i. strain and ii. frequency (N = 3–5). **C)** NO release into media 9 hr post-loading (N = 5). Gene expression 9 hr post-loading of **D)** *Nos2* (N = 5), **E)** *Tnfa* (N = 5), **F)** *Il1b* (N = 5), **G)** *Ifng* (N = 4,5,5,5), **H)** *Tlr4* (N = 4,5,5,5), **I)** *Hmgb1* (N = 5), **J)** *Il6* (N = 5), **K)** *Il10* (N = 5), **L)** *Arg1* (N = 5,5,4,5), in addition to ECM genes **M)** *Col1a1*, *Col2a1*, *Acan*, *Mmp3*, and *Mmp12* (N = 5). $^{****}p < 0.0001$, $^{***}p < 0.001$, $^{**}p < 0.01$, $^{*}p < 0.05$, and $\#p < 0.1$.

In unloaded + TAK242, the NP maintained its round, oval shape (Fig. 6**F-H**) with ~ 60 % of NP cells appearing large and vacuolated (Fig. 6**I**), and AF morphology remained intact. In static + TAK242, NP shape was round and vacuolated, while the AF appeared less distorted than in static. In dynamic + TAK242 loaded discs, there were no qualitative differences observed versus no TAK242 counterparts.

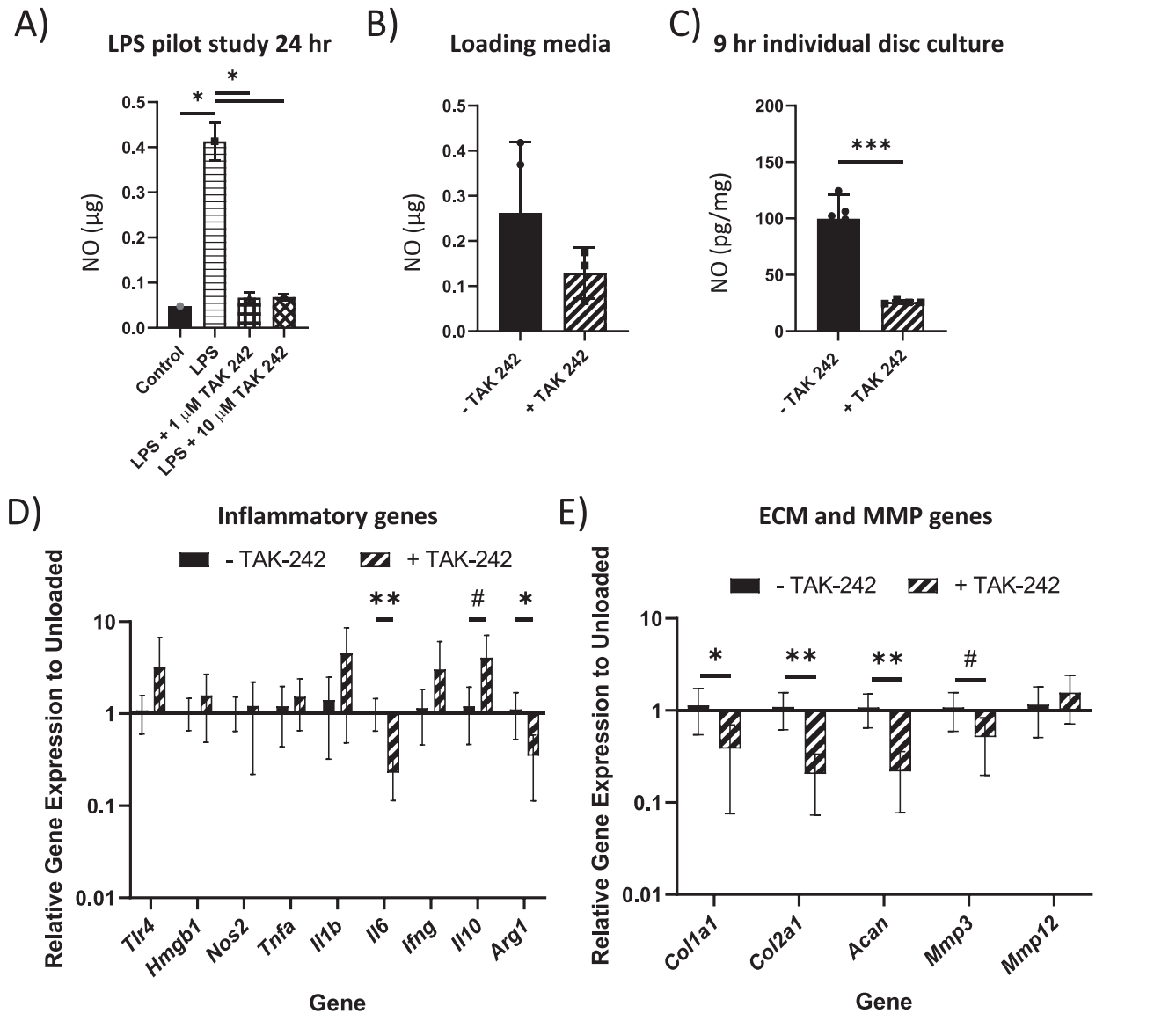

Fig. 4. Effect of TAK-242 on Inflammatory and ECM changes in unloaded discs. A) NO release of unloaded discs stimulated with LPS and cultured with 1 µM or 10 µM TAK-242 for 24 hr (N = 2), **B)** 3 hr NO release into media with unloaded discs ± 1 µM TAK-242 (N = 4,3), and **C)** NO release from individual discs 9 hr post-loading (N = 5). **D)** Inflammatory gene expression (N = 5) and **E)** ECM gene expression 9 hr of unloaded discs ± 1 µM TAK-242 (N = 5). ***$p < 0.001$, **$p < 0.01$, *$p < 0.05$, and #$p < 0.1$.

4. Discussion

The goals of this study were to characterize the inflammatory expression changes in response to static and dynamic loading and to investigate the contributions of TLR4 to mechanically-induced inflammatory signaling using an organ culture model of bone-disc-bone motion segments. NO release into the LM was highly correlated with applied frequency and strain magnitude across different loading profiles. Static and high-dynamic loading significantly increased *Tlr4* and *Hmgb1* gene expression, which was not observed in the more physiologically relevant low-dynamic loading. The current study also investigated the efficacy of TAK-242, a drug that inhibits pro-inflammatory TLR4 signaling. While co-treatment with TAK-242 significantly decreased NO release in unloaded groups, its effects on loaded IVDs differed by loading profiles, where TAK-242 decreased pro-inflammatory expression in static but not dynamic loaded groups. This suggests that TLR4 plays a direct role in mediating inflammatory responses of IVD to static compression.

NO release may also be affected by solute transport associated with different loading profiles. The cyclic nature of dynamic loading may be modulating the transport of cytokines into the media, possibly through convection-aided transport (Ferguson et al., 2004; Walter et al., 2015; Gullbrand et al., 1976). NO release was higher in low- and high-dynamic loading conditions, which may be due to higher NO production and/or greater solute convection at these frequencies. Despite the significant increase in *Nos2* gene expression with static loading, NO media levels did not change, potentially due to the lack of fluid flow convection. Matrix compaction due to static loading may have also hindered the diffusion of NO from disc into the media (Evans & Quinn, 2006). Although motion segments largely recovered back to pre-load height during incubation (**Fig.S3**), NO release during incubation was similar across loading groups. Over time, 5-day loading led to a nonlinear increase in cumulative NO release, driven primarily by increases in NO levels during earlier loading events (**Fig.S1**).

The catabolic IVD tissue response to static and high-dynamic loading suggests that non-physiological loading elicits a similar, molecular profile, including significant increases in *Tnfa* and *Il1b* expression. TNFα

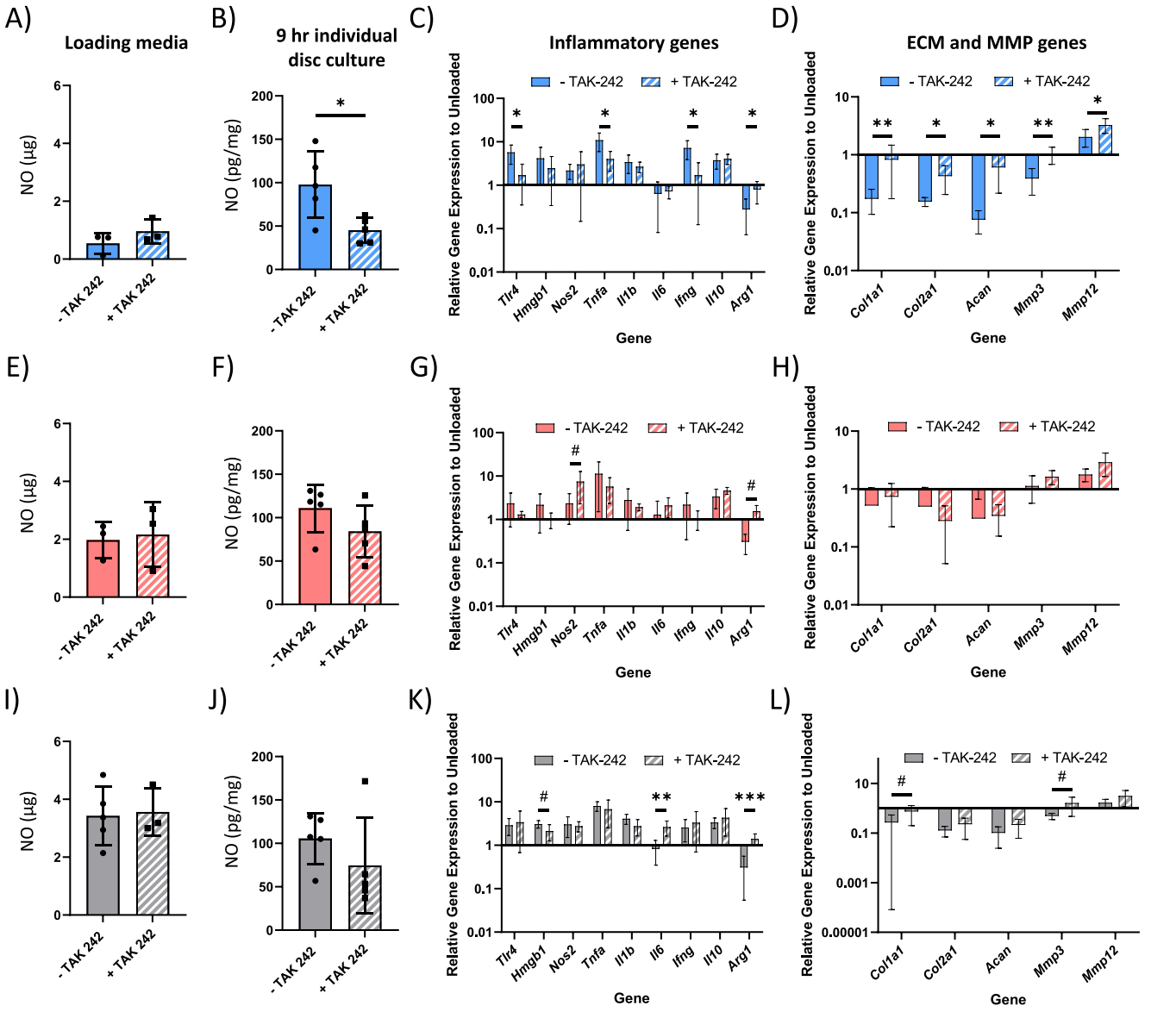

Fig. 5. Effect of TAK242 on Inflammatory and ECM changes in static, low-dynamic, and high-dynamic discs. Static loading ± 1 µM TAK-242 effects on **A)** loading media NO release (N = 3), **B)** incubation media NO release (N = 5), **C)** inflammatory gene expression (N = 4–5), and **D)** ECM gene expression. Low-dynamic loading ± 1 µM TAK-242 effects on **E)** loading media NO release (N = 3), **F)** incubation media NO release (N = 5), **G)** inflammatory gene expression (N = 3–5), and **H)** ECM gene expression (N = 3–5). High-dynamic loading ± 1 µM TAK-242 effects on **I)** loading media NO release (N = 3–5), **J)** incubation media NO release (N = 5), **K)** inflammatory gene expression (N = 4–5), and **L)** ECM gene expression (N = 5). $***p < 0.001$, $**p < 0.01$, $*p < 0.05$, and $\#p < 0.1$.

and IL-1β are key pro-inflammatory cytokines elevated in human samples of degenerated discs (Le Maitre et al., 2007). Though IL-6 is also associated with advanced degeneration (Capossela et al., 2014; Risbud & Shapiro, 2014; Svensson, 2010), significant differences in *Il6* expression were not observed in either short- or long-term loading protocols (**Fig.S1,S2**). TNFα also promotes IL-10 secretion which serves as a negative feedback on pro-inflammatory cytokines to mitigate damage (Wanidworanun and Strober, 1993). Indeed, we observed *Tnfa* upregulation along with *Il10* upregulation in injurious loading conditions. However, the 5-day loading study showed decreased *Tnfa* inflammatory gene expression compared to 1-day loading (**Fig.S2D**), which may be a consequence of IL-10 feedback. Since *Il10* was upregulated in static and high-dynamic loading, this suggests that anti-inflammatory signaling is activated in the same post-loading timeline as pro-inflammatory activation.

Static and high-dynamic loading resulted in similar alterations of pro-inflammatory cytokines and ECM gene expression, whereas the low-dynamic group was considered more physiologically relevant since it did not lead to significant pro-inflammatory upregulation of cytokines. When assessing the impact of loading magnitude, the high-static group also exhibited a similar profile of elevated inflammatory genes to static and high-dynamic groups (**Fig. S4**). Interestingly, *Ifng* expression increased in static and high static, but not high dynamic loading. IFNG is an important mediator of immunity and inflammation (Brierley & Fish, 2002). The results of this study differ from literature which found distinct inflammatory responses to static and dynamic loading. In Wang *et al.,* greater levels of *IL1B* and *TNFA* expression were found under static loading (0.5 MPa) compared to dynamic loading (0.5 – 1.0 MPa with either 0.1 or 1 Hz) (Wang et al., 2007). These findings are consistent with our findings using low-dynamic loading. Some studies show that dynamic loading was more detrimental to IVD integrity than static loading, where higher applied loading frequencies led to greater cell death, which was not examined directly in the current study (Paul et al., 2017; Paul et al., 2013). We observed differences in histological changes

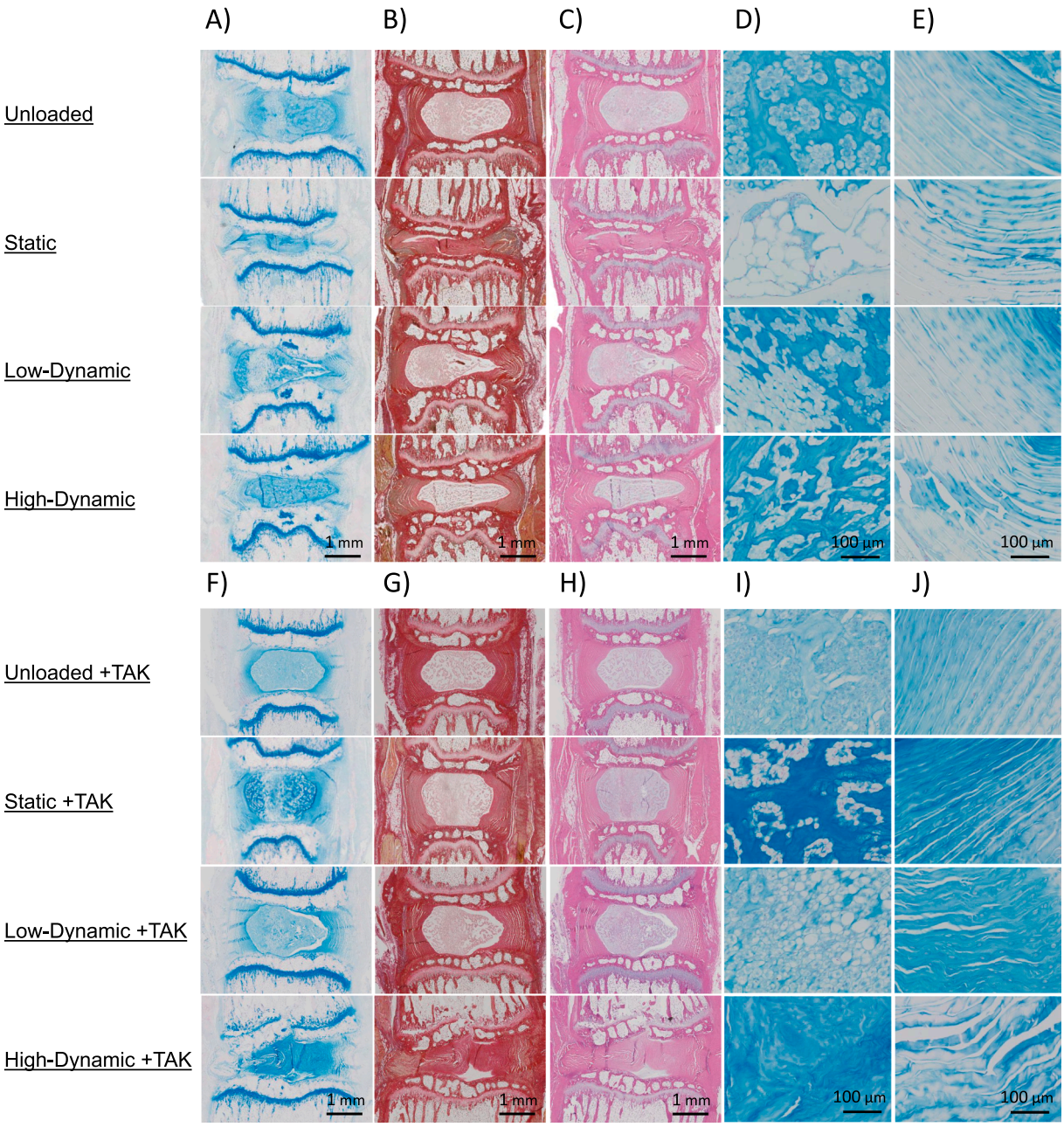

Fig. 6. Effect of TAK-242 on histological changes in loaded discs. Histology on discs post loading **A-E)** without TAK-242 and F-**J)** with TAK-242 from unloaded, static, low-dynamic, and high-dynamic conditions. **A,F)** Alcian Blue, **B,G)** Picrosirius Red, **C,H)** H&E. Higher magnification images of Alcian blue stained slides from the **D,I)** NP region, and **E,J)** AF region. (For interpretation of the references to color in this figure legend, the reader is referred to the web version of this article.)

of the IVD in static and high-dynamic versus unloaded, although their pro-inflammatory profiles were similar. Specifically, static loading led to more morphological disruption than low-and high-dynamic discs versus unloaded discs. This suggests that fluid pressurization from dynamic loading may have protected against NP cell or tissue rupture.

Tlr4 expression was upregulated in static and high-dynamic loading versus unloaded discs. Activation of TLR4 can enhance the production of mediators such as HMGB1 which can also augment the inflammatory response (He et al., 2018; Rajan et al., 2013). High HMGB1 levels can promote GAG loss in discs, which may be contributing to the GAG loss observed in the histological analyses of static and high-dynamic loading (Shah et al. 2019).

The current study also investigated the efficacy of TAK-242, a drug that inhibits intracellular TLR4 signaling and decreases downstream NF-kB activation in response to inflammatory stimuli (Feng et al., 2017; Matsunaga et al., 2011). While co-treatment with TAK-242 post-injury significantly decreased NO release in unloaded discs, its effects on loaded IVD motion segments differed by loading profiles. TAK-242 co-treatment decreased pro-inflammatory expression in unloaded and static, but not dynamic loaded groups, suggesting that TLR4 plays a direct role in mediating inflammatory responses of IVD to static loading. There was a slight qualitative difference in the representative histology of + TAK static loaded discs in which the ECM was better conserved compared to the -TAK counterpart. This is consistent with gene expression results where effects of static loading were mitigated by TAK-242. However, during loading, NO release was not affected by TAK-242. Thus, TLR4 may mediate post-injury, rather than during injury, inflammatory responses. Some possible reasons for this may be that the loading period is too short for the drug to penetrate and influence cells within a compacted ECM during compression.

Findings indicated that TAK-242 effectively mitigated post-injury response when loading increased *Tlr4* levels (i.e. static loading). Indeed, TAK-242 significantly decreased levels of *Tlr4* and decreased pro-inflammatory cytokines *Tnfa* and *Ifng* gene expression under static loading. A concomitant increase in macrophage related factors, *Arg1* and *Mmp12*, was observed in TAK-242 treated static loaded discs. *Col1a1*, *Col2a1*, and *Acan* gene expression also increased significantly with TAK-242, suggesting *Tlr4* inhibition also promoted an anabolic remodeling response due to an increase in *Mmp3* expression. Findings are consistent with our prior study that showed how TAK-242 abrogated HMGB1-induced *MMP1* expression in addition to mitigating NF-κB signaling in human NP cells *in vitro* (Shah et al., 2019). The increase in *Arg1* expression also supports additional anti-inflammatory effects of *Tlr4* inhibition (Adhikari et al., 2007; Matsunaga et al., 2011), further demonstrating the potential of decreasing the pro-inflammatory response to static loading.

Some limitations of this study include the use of discs after soft tissue removal during dissection, discs being exposed to different loading profiles and orientations compared to an *in vivo* setting, and the absence of systemic circulation *in vitro*. Furthermore, gene expression reported in this study represents contributions of heterogenous IVD tissue, including NP, AF, and CEPs, with media analyses including contributions of surrounding vertebral bone. Maintenance of the intact IVD, including uninterrupted CEP to bone interface, was necessary to maintain motion segment integrity for applied loading. We aimed to minimize the potential for herniation of the NP from the loaded IVD by keeping an intact interface with surrounding bone. However, bone presence may have interfered with diffusion of molecules in or out of the tissue.

CRediT authorship contribution statement

Hagar M. Kenawy: Writing – review & editing, Writing – original draft, Visualization, Validation, Methodology, Investigation, Formal analysis, Data curation, Conceptualization. **Samantha L. Marshall:** Writing – review & editing, Methodology, Investigation, Formal analysis, Data curation, Conceptualization. **James Rogot:** Writing – review & editing, Investigation. **Andy J. Lee:** Writing – review & editing, Methodology, Formal analysis. **Clark T. Hung:** Writing – review & editing, Supervision, Project administration, Methodology, Funding acquisition, Formal analysis, Conceptualization. **Nadeen O. Chahine:** Writing – review & editing, Supervision, Project administration, Methodology, Funding acquisition, Formal analysis, Conceptualization.

Declaration of Competing Interest

The authors declare that they have no known competing financial interests or personal relationships that could have appeared to influence the work reported in this paper.

Acknowledgements

This study was supported in part by NIH R01AR069668, R01AR077760, R21AR080516, and P41EB027062.. We would like to thank the histology services at Molecular Pathology Shared Resource (MPSR) located at the Columbia University Irving Medical Center (CUIMC). We would also like to thank Microsurgery Research and Training Lab Co-Director Yelena Akelina DVM, MS for donating fresh rat cadavers for experiments.

Appendix A. Supplementary data

Supplementary data to this article can be found online at https://doi.org/10.1016/j.jbiomech.2023.111491.

References

Adhikari, A., Xu, M., Chen, Z.J., 2007. Ubiquitin-mediated activation of TAK1 and IKK. Oncogene 26 (22), 3214–3226. https://doi.org/10.1038/sj.onc.1210413.

Baer, A.E., Laursen, T.A., Guilak, F., Setton, L.A., 2003. The micromechanical environment of intervertebral disc cells determined by a finite deformation, anisotropic, and biphasic finite element model. J. Biomech. Eng. 125 (1), 1–11. https://doi.org/10.1115/1.1532790.

Best, B.A., Guilak, F., Setton, L.A., Zhu, W., Saed-Nejad, F., Ratcliffe, A., Weidenbaum, M., Mow, V.C., 1994. Compressive mechanical properties of the human anulus fibrosus and their relationship to biochemical composition. Spine 19 (2), 212–221. https://doi.org/10.1097/00007632-199401001-00017.

Brierley, M.M., Fish, E.N., 2002. Review: IFN-alpha/beta receptor interactions to biologic outcomes: understanding the circuitry. J. Interferon Cytokine Res.: Offic. J Int. Soc. Interferon Cytokine Res. 22 (8), 835–845. https://doi.org/10.1089/107999002760274845.

Capossela, S., Schlafli, P., Bertolo, A., Janner, T., Stadler, B.M., Potzel, T., Baur, M., Stoyanov, J.V., 2014. Degenerated human intervertebral discs contain autoantibodies against extracellular matrix proteins. discussion 263 Eur. Cell Mater. 27, 251–263. https://doi.org/10.22203/ecm.v027a18.

Christ, W., Dupuis, H., 1966. [On the stressing of the spine under the effect of sinusoidal and stochastic vibrations]. Int Z Angew Physiol 22 (3), 258–278.

Dunstan, D.W., Howard, B., Healy, G.N., Owen, N., 2012. Too much sitting – A health hazard. Diabetes Res. Clin. Pract. 97 (3), 368–376. https://doi.org/10.1016/j.diabres.2012.05.020.

Evans, R.C., Quinn, T.M., 2006. Dynamic Compression Augments Interstitial Transport of a Glucose-Like Solute in Articular Cartilage. Biophys. J . 91 (4), 1541–1547. https://doi.org/10.1529/biophysj.105.080366.

Fang, F., Jiang, D., 2016. IL-1β/HMGB1 signalling promotes the inflammatory cytokines release via TLR signalling in human intervertebral disc cells. Biosci. Rep. 36 (5) https://doi.org/10.1042/BSR20160118.

Feng, Y., Gao, J., Cui, Y., Li, M., Li, R., Cui, C., Cui, J., 2017. Neuroprotective Effects of Resatorvid Against Traumatic Brain Injury in Rat: Involvement of Neuronal Autophagy and TLR4 Signaling Pathway. Cell. Mol. Neurobiol. 37 (1), 155–168. https://doi.org/10.1007/s10571-016-0356-1.

Ferguson, S.J., Ito, K., Nolte, L.P., 2004. Fluid flow and convective transport of solutes within the intervertebral disc. J Biomech 37 (2), 213–221. https://doi.org/10.1016/s0021-9290(03)00250-1.

Frymoyer, J.W., Cats-Baril, W.L., 1991. An overview of the incidences and costs of low back pain. Orthop. Clin. North Am. 22 (2), 263–271.

Gu, W.Y., Yao, H., 2003. Effects of hydration and fixed charge density on fluid transport in charged hydrated soft tissues. Ann. Biomed. Eng. 31 (10), 1162–1170. https://doi.org/10.1114/1.1615576.

Gullbrand, S.E., Peterson, J., Ahlborn, J., et al., 2015. ISSLS Prize Winner: Dynamic Loading-Induced Convective Transport Enhances Intervertebral Disc Nutrition. Spine (Phila Pa 1976) 40 (15), 1158–1164. https://doi.org/10.1097/BRS.0000000000001012.

He, M., Bianchi, M.E., Coleman, T.R., Tracey, K.J., Al-Abed, Y., 2018. Exploring the biological functional mechanism of the HMGB1/TLR4/MD-2 complex by surface plasmon resonance. Mol. Med. 24 (1), 21. https://doi.org/10.1186/s10020-018-0023-8.

Healy, G.N., Matthews, C.E., Dunstan, D.W., Winkler, E.A.H., Owen, N., 2011. Sedentary time and cardio-metabolic biomarkers in US adults: NHANES 2003–06. Eur. Heart J. 32 (5), 590–597. https://doi.org/10.1093/eurheartj/ehq451.

Huang, C.Y., Gu, W.Y., 2008. Effects of mechanical compression on metabolism and distribution of oxygen and lactate in intervertebral disc. J. Biomech. 41 (6), 1184–1196. https://doi.org/10.1016/j.jbiomech.2008.02.002.

Iatridis, J.C., Setton, L.A., Foster, R.J., Rawlins, B.A., Weidenbaum, M., Mow, V.C., 1998. Degeneration affects the anisotropic and nonlinear behaviors of human anulus fibrosus in compression. J. Biomech. 31 (6), 535–544. https://doi.org/10.1016/s0021-9290(98)00046-3.

Kelly, T.-A.-N., Fisher, M.B., Oswald, E.S., Tai, T., Mauck, R.L., Ateshian, G.A., Hung, C. T., 2008. Low-Serum Media and Dynamic Deformational Loading in Tissue Engineering of Articular Cartilage. Ann. Biomed. Eng. 36 (5), 769–779. https://doi.org/10.1007/s10439-008-9476-1.

Klawitter, M., Hakozaki, M., Kobayashi, H., Krupkova, O., Quero, L., Ospelt, C., Gay, S., Hausmann, O., Liebscher, T., Meier, U., Sekiguchi, M., Konno, S.-I., Boos, N., Ferguson, S.J., Wuertz, K., 2014. Expression and regulation of toll-like receptors (TLRs) in human intervertebral disc cells. Eur. Spine J. 23 (9), 1878–1891. https://doi.org/10.1007/s00586-014-3442-4.

Korecki, C.L., Kuo, C.K., Tuan, R.S., Iatridis, J.C., 2009. Intervertebral disc cell response to dynamic compression is age and frequency dependent. J. Orthop. Res. 27 (6), 800–806. https://doi.org/10.1002/jor.20814.

Krock, E., Rosenzweig, D.H., Currie, J.B., Bisson, D.G., Ouellet, J.A., Haglund, L., 2017. Toll-like Receptor Activation Induces Degeneration of Human Intervertebral Discs. Sci. Rep. 7 (1), 17184. https://doi.org/10.1038/s41598-017-17472-1.

Lang, G., Liu, Y., Geries, J., Zhou, Z., Kubosch, D., Südkamp, N., Richards, R.G., Alini, M., Grad, S., Li, Z., 2018. An intervertebral disc whole organ culture system to investigate proinflammatory and degenerative disc disease condition. J. Tissue Eng. Regen. Med. 12 (4), e2051–e2061. https://doi.org/10.1002/term.2636.

Le Maitre, C.L., Hoyland, J.A., Freemont, A.J., 2007. Catabolic cytokine expression in degenerate and herniated human intervertebral discs: IL-1β and TNFα expression profile. Arthritis Res. Ther. 9 (4), R77. https://doi.org/10.1186/ar2275.

Le Maitre, C.L., Frain, J., Fotheringham, A.P., Freemont, A.J., Hoyland, J.A., 2008. Human cells derived from degenerate intervertebral discs respond differently to those derived from non-degenerate intervertebral discs following application of

dynamic hydrostatic pressure. Biorheology 45 (5), 563–575. https://doi.org/10.3233/BIR-2008-0498.
Le Maitre, C.L., Frain, J., Millward-Sadler, J., Fotheringham, A.P., Freemont, A.J., Hoyland, J.A., 2009. Altered integrin mechanotransduction in human nucleus pulposus cells derived from degenerated discs. Arthritis Rheum. 60 (2), 460–469. https://doi.org/10.1002/art.24248.
MacLean, J.J., Lee, C.R., Grad, S., Ito, K., Alini, M., & Iatridis, J.C., 2003. Effects of Immobilization and Dynamic Compression on Intervertebral Disc Cell Gene Expression In Vivo. SPINE, 28, 10, 973–981. https://doi.org/10.1097/01.BRS.0000061985.15849.A9.
MacLean, J.J., Lee, C.R., Alini, M., Iatridis, J.C., 2004. Anabolic and catabolic mRNA levels of the intervertebral disc vary with the magnitude and frequency of in vivo dynamic compression. J. Orthopaedic Res. 22 (6), 1193–1200. https://doi.org/10.1016/j.orthres.2004.04.004.
Maclean, J.J., Lee, C.R., Alini, M., Iatridis, J.C., 2005. The effects of short-term load duration on anabolic and catabolic gene expression in the rat tail intervertebral disc. J. Orthop. Res. 23 (5), 1120–1127. https://doi.org/10.1016/j.orthres.2005.01.020.
Magnusson, M., 1992. Measurement of Height Loss During Whole Body Vibrations. J. Spinal Disord. 5 (2), 198–203. https://doi.org/10.1097/00002517-199206000-00009.
Maidhof, R., Jacobsen, T., Papatheodorou, A., Chahine, N.O., Kletsas, D., 2014. Inflammation induces irreversible biophysical changes in isolated nucleus pulposus cells. PLoS One 9 (6), e99621.
Matsunaga, N., Tsuchimori, N., Matsumoto, T., Ii, M., 2011. TAK-242 (Resatorvid), a Small-Molecule Inhibitor of Toll-Like Receptor (TLR) 4 Signaling, Binds Selectively to TLR4 and Interferes with Interactions between TLR4 and Its Adaptor Molecules. Mol. Pharmacol. 79 (1), 34–41. https://doi.org/10.1124/mol.110.068064.
Matthews, C.E., Chen, K.Y., Freedson, P.S., Buchowski, M.S., Beech, B.M., Pate, R.R., Troiano, R.P., 2008. Amount of Time Spent in Sedentary Behaviors in the United States, 2003–2004. Am. J. Epidemiol. 167 (7), 875–881. https://doi.org/10.1093/aje/kwm390.
Motulsky, H.J., Brown, R.E., 2006. Detecting outliers when fitting data with nonlinear regression – a new method based on robust nonlinear regression and the false discovery rate. BMC Bioinformatics 7 (1), 123. https://doi.org/10.1186/1471-2105-7-123.
Nachemson, A.L., 1981. Disc pressure measurements. Spine 6 (1), 93–97. https://doi.org/10.1097/00007632-198101000-00020.
O'Connell, G.D., Johannessen, W., Vresilovic, E.J., Elliott, D.M., 2007. Human internal disc strains in axial compression measured noninvasively using magnetic resonance imaging. Spine 32 (25), 2860–2868. https://doi.org/10.1097/BRS.0b013e31815b75fb.
O'Connell, G.D., Vresilovic, E.J., Elliott, D.M., 2011. Human intervertebral disc internal strain in compression: The effect of disc region, loading position, and degeneration. J. Orthop. Res. 29 (4), 547–555. https://doi.org/10.1002/jor.21232.
Paul, C.P.L., Schoorl, T., Zuiderbaan, H.A., Zandieh Doulabi, B., van der Veen, A.J., van de Ven, P.M., Smit, T.H., van Royen, B.J., Helder, M.N., Mullender, M.G., Kletsas, D., 2013. Dynamic and Static Overloading Induce Early Degenerative Processes in Caprine Lumbar Intervertebral Discs. PLoS One 8 (4), e62411.
Paul, C.P.L., de Graaf, M., Bisschop, A., Holewijn, R.M., van de Ven, P.M., van Royen, B. J., Mullender, M.G., Smit, T.H., Helder, M.N., Chung, C.K., 2017. Static axial overloading primes lumbar caprine intervertebral discs for posterior herniation. PLoS One 12 (4), e0174278.
Pope, M.H., Magnusson, M., Wilder, D.G., 1998. Low Back Pain and Whole Body Vibration. Clin. Orthop. Relat. Res. 354, 241–248. https://doi.org/10.1097/00003086-199809000-00029.
Quero, L., Klawitter, M., Schmaus, A., Rothley, M., Sleeman, J., Tiaden, A.N., Klasen, J., Boos, N., Hottiger, M.O., Wuertz, K., Richards, P.J., 2013. Hyaluronic acid fragments enhance the inflammatory and catabolic response in human intervertebral disc cells through modulation of toll-like receptor 2 signalling pathways. Arthritis Res. Ther. 15 (4), R94. https://doi.org/10.1186/ar4274.
Rajan, N.E., Bloom, O., Maidhof, R., Stetson, N., Sherry, B., Levine, M., Chahine, N.O., 2013. Toll-Like Receptor 4 (TLR4) Expression and Stimulation in a Model of Intervertebral Disc Inflammation and Degeneration. Spine 38 (16), 1343–1351. https://doi.org/10.1097/BRS.0b013e31826b71f4.
Ravindra, V.M., Senglaub, S.S., Rattani, A., Dewan, M.C., Härtl, R., Bisson, E., Park, K.B., Shrime, M.G., 2018. Degenerative Lumbar Spine Disease: Estimating Global Incidence and Worldwide Volume. Glob. Spine J. 8 (8), 784–794. https://doi.org/10.1177/2192568218770769.
Risbud, M.V., Shapiro, I.M., 2014. Role of cytokines in intervertebral disc degeneration: pain and disc content. Nat. Rev. Rheumatol. 10 (1), 44–56. https://doi.org/10.1038/nrrheum.2013.160.
Salvatierra, J.C., Yuan, T.Y., Fernando, H., Castillo, A., Gu, W.Y., Cheung, H.S., Huant, C.-Y.-C., 2011. Difference in Energy Metabolism of Annulus Fibrosus and Nucleus Pulposus Cells of the Intervertebral Disc. Cell. Mol. Bioeng. 4 (2), 302–310. https://doi.org/10.1007/s12195-011-0164-0.
Sandover, J., 1983. Dynamic Loading as a Possible Source of Low-Back Disorders. Spine 8 (6), 652–658.
Schneider, C.A., Rasband, W.S., Eliceiri, K.W., 2012. NIH Image to ImageJ: 25 years of image analysis. Nat. Methods 9 (7), 671–675. https://doi.org/10.1038/nmeth.2089.
Schultz, A.B., Warwick, D.N., Berkson, M.H., Nachemson, A.L., 1979. Mechanical Properties of Human Lumbar Spine Motion Segments—Part I: Responses in Flexion, Extension, Lateral Bending, and Torsion. J. Biomech. Eng. 101 (1), 46–52. https://doi.org/10.1115/1.3426223.
Setton, L.A., Chen, J., 2006. Mechanobiology of the intervertebral disc and relevance to disc degeneration. J. Bone Joint Surg. Am. 88 (Suppl 2), 52–57. https://doi.org/10.2106/JBJS.F.00001.
Shah, B.S., Burt, K.G., Jacobsen, T., Fernandes, T.D., Alipui, D.O., Weber, K.T., Levine, M., Chavan, S.S., Yang, H., Tracey, K.J., Chahine, N.O., 2019. High mobility group box-1 induces pro-inflammatory signaling in human nucleus pulposus cells via toll-like receptor 4-dependent pathway. J. Orthop. Res. 37 (1), 220–231. https://doi.org/10.1002/jor.24154.
Svensson, C.I., 2010. Interleukin-6: a local pain trigger? Arthritis Res. Ther. 12 (5), 145. https://doi.org/10.1186/ar3138 ar3138.
Walsh, A.J.L., Lotz, J.C., 2004. Biological response of the intervertebral disc to dynamic loading. J. Biomech. 37 (3), 329–337. https://doi.org/10.1016/S0021-9290(03)00290-2.
Walter, B.A., Likhitpanichkul, M., Illien-Junger, S., Roughley, P.J., Hecht, A.C., Iatridis, J.C., 2015. TNFα transport induced by dynamic loading alters biomechanics of intact intervertebral discs. PLoS One 10 (3), e0118358. https://doi.org/10.1371/journal.pone.0118358.
Wang, D.-L., Jiang, S.-D., Dai, L.-Y., 2007. Biologic response of the intervertebral disc to static and dynamic compression in vitro. Spine 32 (23), 2521–2528. https://doi.org/10.1097/BRS.0b013e318158cb61.
Wanidworanun, C., & Strober, W., 1993. Predominant role of tumor necrosis factor-alpha in human monocyte IL-10 synthesis. J. Immunol., 151, 12, 6853–6861.
Wilder, D., Pope, M., 1996. Epidemiological and aetiological aspects of low back pain in vibration environments—an update. Clin. Biomech. 11 (2), 61–73. https://doi.org/10.1016/0268-0033(95)00039-9.
Wilke, H.-J., Neef, P., Caimi, M., Hoogland, T., Claes, L.E., 1999. New In Vivo Measurements of Pressures in the Intervertebral Disc in Daily Life. Spine 24 (8), 755–762.
Wuertz, K., Godburn, K., MacLean, J.J., Barbir, A., Donnelly, J.S., Roughley, P.J., Alini, M., Iatridis, J.C., 2009. In vivo remodeling of intervertebral discs in response to short- and long-term dynamic compression. J. Orthop. Res. 27 (9), 1235–1242. https://doi.org/10.1002/jor.20867.
Yao, H., Gu, W.Y., 2006. Physical signals and solute transport in human intervertebral disc during compressive stress relaxation: 3D finite element analysis. Biorheology 43 (3,4), 323–335.
Zhou, Z., Cui, S., Du, J., et al., 2021. One strike loading organ culture model to investigate the post-traumatic disc degenerative condition. J. Orthop. Translat. 26, 141–150. https://doi.org/10.1016/j.jot.2020.08.003.